Spectral Influences on Performance: A South African PV Plant after 4 years of operation

Francisca M. Daniel-Durandt
Dr. Arnold J. Rix
Stellenbosch University
18296033@sun.ac.za

Abstract
The performance ratio (PR) of a South African photovoltaic (PV) plant, over 4 operational years, is discussed by assessing the normal and weather-corrected PR calculation under well-known spectral influences, being airmass (AM) and precipitable water (PW). The PR is determined for different intervals of AM and PW to identify scenarios in which the normal and weather-corrected PR shows significant deviations. The spectral irradiance of polycrystalline PV modules is simulated for different AM and PW values to identify the wavelengths where the PV module underperforms. Both the normal and weather-corrected PR is decreased when AM levels are higher than 3, PW is greater than 0.8 cm, and calculated cell temperatures below 30℃. The corrected PR is more stable for ideal operating conditions but shows significant deviations under nonideal circumstances. The spectrum is affected in the 0.9 to 1.0 µm wavelengths for changes from standard testing conditions in both the AM and PW. Changes in AM have a greater effect on spectral irradiance in the 0.7 to 0.8 µm wavelengths. The PV module's spectral response is higher in the 0.7 to 1.0 µm wavelengths, which results in a more pronounced effect on performance.

Keywords: Performance ratio, weather-corrected performance ratio, airmass, precipitable water, spectrum

1. Introduction

The majority of the global civilisation produces electricity using fossil fuels such as coal, oil, and natural as the main source. However, the emissions of chemical compounds produced by these sources contribute to the acceleration of climate change (Gouvêa, et al., 2017).

The low-carbon energy revolution is led primarily by photovoltaic (PV) technology and is becoming one of the most affordable energy resources for most countries. PV plants usually have a 25-year design life and the operation and maintenance play an important role in how successful the plant will be over that lifetime (Gopi, et al., 2021).

PV module degradation is a gradual deterioration that affects the operational capability of the PV module within acceptable limits. Africa has the poorest representation in the literature on the reporting degradation rate. Development in Sub-Saharan Africa and East Africa is laggard to the rest of the continent, and this is attributed to the lack of data on different types of climates in these regions (Daher, et al., 2022).

The performance ratio (PR) is used as a metric for determining the degradation rate of a PV plant, as well as being an important assessment tool in a PV system's performance (Gopi, et al., 2021). PR measures overall efficiency and indicates how well the system compares with the ideal performance (Daher, et al., 2022). A standard spectral irradiance was defined by the scientific community as a reference when determining the power ratings of PV modules. These conditions are called standard testing conditions (STC) (Rodrigo, et al., 2019). STC conditions are defined as 1000 W/m^2 irradiance, 25℃ cell temperature, and airmass (AM) 1.5, which is the standard/reference spectrum (Gouvêa, et al., 2017).

The reference spectrum is usually replicated in a controlled environment, which creates difficulty in replicating the STC conditions in real outdoor operating conditions (Rodrigo, et al., 2019). In addition, the atmosphere changes over the course of a day and over seasons.

In general, the PV modules do not correspond to the full AM 1.5 spectrum (Gouvêa, et al., 2017). Atmospheric conditions cause variations in spectral irradiance due to the scattering and absorption phenomenon and the three main weather variables are the AM, aerosol optical depth (AOD), and precipitable water (PW). All three of these variables change over the course of a day and seasons (Rodrigo, et al., 2019; Gouvêa, et al., 2017) and for clear sky conditions, the AM, AOD, and PW contribute more to the changes in the spectrum. Unrealistic yield predictions are obtained when the changes in the spectrum's distribution are ignored (Caballero, et al., 2018).

Despite these spectral influences, the PR has not yet been adjusted to account for the previously discussed influences. NREL has proposed the weather-corrected performance ratio (WC-PR) (Dierauf, et al., 2013; Gopi, et al., 2021), which corrects the PR for influences of irradiance and temperature.

Ground-based solar spectrum measurements are scarce, costly, and require high maintenance (Caballero, et al., 2018). Satellite-based modelled data have been used to map annual average spectral influences over large geographical areas; however, these simulation techniques require further experimental validation (Caballero, et al., 2018).

Correction methodologies for the spectrum have been defined separately by several authors. Corrections using AM and the clearness index have been proposed by Martin & Ruiz (1999), which was further taken by Gottschalg, et al. (2004) using AM and a modified clearness index for modules of crystalline silicon (c-Si) and amorphous silicon (a-Si). However, the model fails to capture seasonal variations (Duck & Fell, 2015; Caballero, et al., 2018).

Further improvements to this model using PW have been proposed; however, this method still depends on the site, raising questions about the universal application of the model (Duck & Fell, 2016; Caballero, et al., 2018). Promising corrections for defining an analytical equation between the spectral mismatch with AM and PW have been proposed by Lee & Panchula (2016), however, the literature is only validated for mono-crystalline (mono-Si) and cadmium telluride (CdTe) (Caballero, et al., 2018). Sandia Labs has proposed a fourth-order polynomial called the airmass function (King, et al., 2004) which is simple and convenient; however, the literature also suggests that the spectral effects in thin-film technologies are not primarily driven by AM (Caballero, et al., 2018). In addition, AM is seasonal and time-of-day dependent.

A mismatch factor analytical equation as a function of AM, AOD, and PW has been proposed by Caballero, et al. (2018) for six different PV technologies. The method models the spectral effects of single junction solar cells and considers the three main influences of the spectrum under clear sky conditions (Caballero, et al., 2018). Their proposed spectral mismatch function outperforms the Sandia Lab airmass function (from King, et al. (2004)), however, requires further validation for universal application (Caballero, et al., 2018).

There is uncertainty as to whether these correction methodologies could be applied to the PR to ensure a more accurate performance representation of the PV plant. In addition, degradation rates and losses should also be considered to exclude any bias it might have with the spectrum.

This article will assess the PR and WC-PR changes for a large-scale PV system with respect to AM and PW over the course of a four-year operational period.

2. Literature Review

2.1. Performance Ratio

2.1.1. Normal PR

Normal PR is calculated using the following:

$$PR_{Normal} = \frac{\sum_i EN_{ac,i}}{\sum_i \left(P_{STC} \cdot \frac{G_{POA,i}}{G_{STC}} \right)}$$

where $EN_{ac,i}$ (kWh) is the measured generation of energy from alternating current (AC), P_{STC} (kW) is the sum of the nameplate ratings for all modules installed in given power blocks during the acceptance test, $G_{POA,i}$ is the measured plane-of-array (POA) irradiance averaged over the time step i (W/m^2) and G_{STC} is the reference irradiance (1000 W/m^2) (Dierauf, et al., 2013; International Electrotechnical Commission, 2021).

2.1.2. NREL Weather Corrected Performance Ratio

WC-PR was developed by NREL, which is more specific to a geographical location (Dierauf, et al., 2013; Gopi, et al., 2021). The methodology accounts for the effects of ambient temperature, wind and solar radiation on the performance of the PV module. The WC-PR is given as

$$PR_{WC} = \frac{\sum_i EN_{ac,i}}{\sum_i \left(P_{STC} \cdot \frac{G_{POA,i}}{G_{STC}} \cdot \left(1 - \frac{\delta}{100} \left(T_{cell,type,avg} - T_{cell,i} \right) \right) \right)}$$

where T_{cell} is the cell temperature calculated from measured meteorological data and δ is the temperature coefficient for power (%/℃, negative in sign).

T_{cell} is calculated using:

$$T_{cell,calc} = T_m + \frac{G_{POA}}{G_{STC}} \times \Delta T$$

where ΔT denotes the conduction temperature drop and T_m is the back-surface temperature of the module, given as:

$$T_m = G_{POA} \times e^{a + b \times WS} + T_a.$$

T_a is the ambient temperature, $e^{a + b \times WS}$ is the conduction/convection heat transfer coefficient empirically determined and WS is the wind speed at the location of the PV power plant, while a, b and ΔT are recommendations of (King, et al., 2004).

Finally, $T_{cell,typ,avg}$ is the average cell temperature weighted by irradiance of one year of weather data and is calculated using the following:

$$T_{cell,typ,avg} = \frac{\sum_j \left[G_{POA,typ,j} \times T_{cell,type,j} \right]}{\sum_j G_{POA,typ,j}}$$

$G_{POA,typ,j}$ and $T_{cell,typ,j}$ are the POA irradiance and calculated cell operating temperature for each hour.

2.2. Spectral Influences

The spectral influences which can be calculated from typical meteorological data are the AM and PW. AM can be calculated from the solar position and PW can be calculated from the relative humidity and temperature (Gueymard, 1993; Gueymard, 1994; Lewis, 2021).

2.2.1. Airmass

AM quantifies the increased amount of substance traversed by the solar rays with respect to a vertical trajectory and is calculated using the solar zenith angle.

AM was defined in (Kasten & Young, 1989) as:

$$AM = \frac{1}{\cos\theta_s \ + \ 0.5057 \cdot \ (\ 96.080 \ - \theta_Z)^{-1.634}}$$

and the absolute airmass (AM_a) can be adjusted for air pressure:

$$AM_a \ = \ AM \cdot \frac{P}{P_o}$$

where P and P_o are the atmospheric pressure at the test site and sea level respectively.

An increase in AM produces strong attenuation in the ultraviolet (UV)-spectrum region and a red shift of spectral distribution. When AM increases, the sun rays traverse a longer trajectory through the atmosphere, which occurs at sunrise and sunset, in winter seasons, and also at higher latitudes.

2.2.2. Precipitable Water

PW accounts for the presence of water vapour in the atmosphere. An increase in PW produces significant attenuation in the near-infrared region on the spectrum which causes a blue shift in the distribution. PW can be estimated from relative humidity and temperature (Gueymard, 1993; Gueymard, 1994; Lewis, 2021):

$$PW \ = \ 0.1 \, H_v \cdot \ \rho_v$$

where H_v is apparent water vapour scale height (km) and ρ_v is the surface water vapour density ($cm^2 \cdot \ g^{-3}$).

$$\rho_v \ = \ 216.7 \cdot \ RH \cdot \frac{e_s}{T}$$

where RH is the relative humidity, e_s is the saturation water vapour pressure and T is the temperature in Kelvin.

H_v is calculated using the following equation:

$$H_v = \ 0.4976 \ + \ 1.5265 \left(\frac{T}{T_0}\right) + \ \exp\left(\ 13.6897 \left(\frac{T}{T_0}\right) \ - \ 14.9188 \left(\frac{T}{T_0}\right)^3 \ \right)$$

where $T_0 \ = \ 273.15$ is the standard temperature in Kelvin.

The most accurate polynomial to estimate e_s is:

$$e_s \ = \sum_{i=0}^{7} b_i \cdot \ T^i$$

where the coefficients are $b_0 \ = \ 6.1104546$, $b_1 \ = \ 0.4442351$, $b_2 = \ 1.402099 \times \ 10^{-2}$, $b_3 = \ 2.6454708 \times \ 10^{-4}$, $b_4 = \ 3.0357098 \times \ 10^{-6}$, $b_5 \ = \ 2.0972268 \times \ 10^{-8}$, $b_6 \ = \ 6.0487594 \times \ 10^{-11}$ and $b_7 = \ -1.469687 \times \ 10^{-13}$ (Gueymard, 1993; Gueymard, 1994; Lewis, 2021).

3. Site Description

The utility-scale PV Plant is based in South Africa. Figure 1 shows the South African map with the GHI penetration levels (Solargis, 2022). The red indicates higher irradiance levels and the green/blue indicates lower irradiance levels. The PV plant is located in the Northern Cape which has an abundance of irradiance. The location and specifics of the PV plant cannot be publicly disclosed. The modules are facing north and fixed at a 30° tilt angle.

There is no intermodule shading that occurs during primary power production hours. The temperatures are high during the summer (December to February) and lower during winter (June to August) where nighttime temperature values can be around 2 ℃. The rainfall period is from February to April, the wind is nearly constant and the site has relatively low humidity levels.

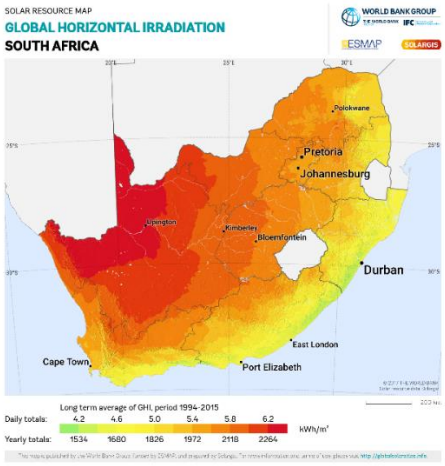

Figure 1: Solar Resource Map of South African indicating GHI penetration levels (Solargis, 2022)

5-minutely data from 01-06-2015 to 31-05-2019 are used for this paper. The dataset is divided into four years, each year spanning from 1 June to 31 May, with missing data from 26 October 2015 to 16 December 2015. For this paper, year 1 is defined from 1 June 2015 to 31 May 2016, year 2 is from 1 June 2016 to 31 May 2017, etc.

The irradiance measurement equipment is EK0 MS-802 pyranometers. A validation study of the observed differences between the measured and other data sources showed that the differences are within a reasonable range.

Figure 2 shows the mean monthly POA irradiance, GHI, and PV power generated over four years. The GHI follows a trend of higher irradiance levels during the Southern Hemisphere summer months (November to February) and lower during the winter months (June to August). Higher POA irradiance levels are observed from August to October, which is associated with higher PV power generation.

From (King, et al., 2004), the a, b and ΔT values are -3.56, -0.075 and 3 for a glass/cell/polymer sheet on an open rack mounting structure. Figure 3 shows the mean monthly $T_{cell,calc}$ and measured module temperatures, as well as the ambient temperature and wind speed. $T_{cell,calc}$ trends slightly higher than the module temperature. The wind speed, also shown in Figure 3, shows a trend similar to the temperature.

Figure 4 shows the mean monthly pressure and humidity. During August to December, lower humidity levels are observed, followed by higher humidity levels from February to July. The pressure follows a similar trend to the humidity. Lower humidity is associated with clearer skies, as also observed in Figure 2 where the GHI is higher during the months when the humidity is lower (October to January).

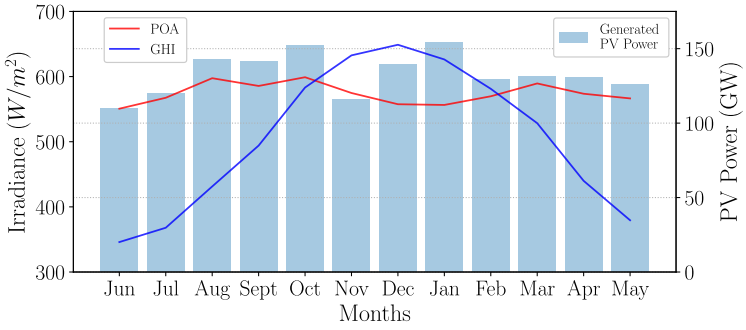

Figure 2: POA Irradiance and PV Power Summary

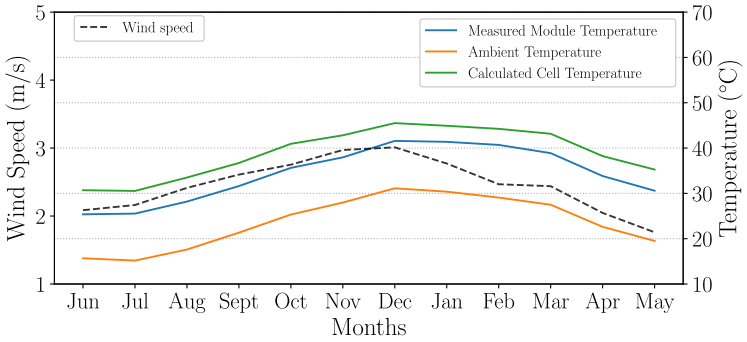

Figure 3: Temperature and Wind Speed Summary

4. Performance Analysis

4.1. Normal and Weather-Corrected Performance Ratio

Figure 5 shows the monthly PR and WC-PR for each year. The normal PR shows greater deviations than the WC-PR, as expected. From April to September, a higher normal PR is calculated, and the PR drops from October to February.

The Southern Hemisphere's summer months are December to February, which is also associated with higher temperatures that is known to reduce PV performance. The WC-PR shows the correction for the winter months (June to August) as lower than the normal PR and then again higher for the summer months. This results in a more stable PR for the entire year with fewer fluctuations. This is also evident when calculating hourly PR and WC-PR.

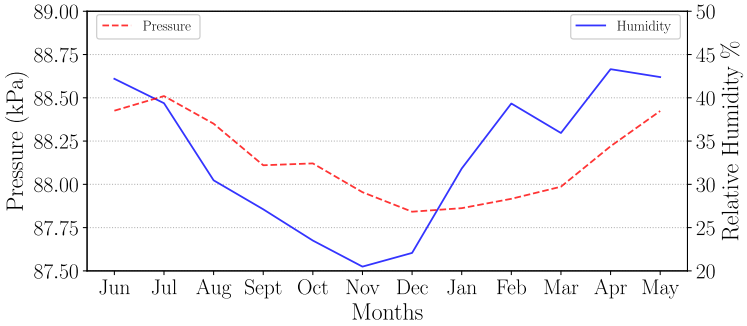

Figure 4: Pressure and Humidity Summary

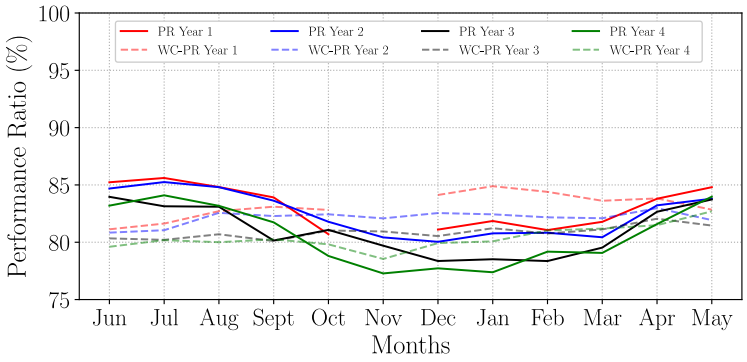

Figure 5: Monthly PR for 4 years

Figure 6 shows the hourly normal and WC-PR for year 1. The red (WC-PR) shows a more stable PR compared to the normal PR. The normal and WC-PR for Year 1 are calculated as 83.2%. A similar trend was noticed for all the years. Normal and WC-PR for year 2 are calculated as 82.2%. Year 3's PR is calculated as 80.9%. Both the normal and WC-PR for Year 4 is calculated as 80.3%. The annual degradation rate R_d is calculated as $-0.9495 \pm 0.405\%$ per year.

4.2. Spectral Influences and Performance Ratio

In Figure 7, the normal PR is indicated with the solid line and the WC-PR is indicated by the dashed line. The data is binned into 200 W/m^2-intervals, therefore 0-200 indicates all timestamps where the POA irradiance was between 0 and 200 W/m^2. Below POA irradiance levels of 400 W/m^2 the PR is underperforming. From 400 to 1200 W/m^2, the WC-PR is quite stable, while the normal PR overestimates the lower levels of POA (400-800) and underestimates the higher levels of POA (1000-1200). The WC-PR is more stable (ie, similar to the annual PR) for 400 to 1200 W/m^2 than the normal PR. There is a slight decrease in performance for POA levels greater than 1200 W/m^2.

In Figure 8, the calculated cell temperature (which is used to calculate WC-PR) is sorted into 15 ℃ intervals. Below 30℃, the PR is significantly lower. As with the POA, the WC-PR is more stable than the normal PR for certain intervals, in this case, for 30 to 75℃. Lower cell temperatures show lower PR.

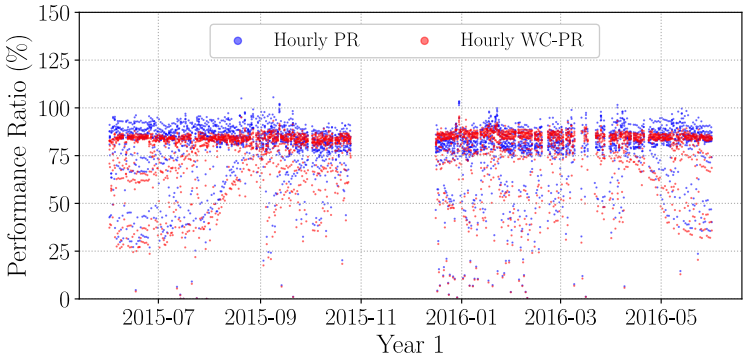

Figure 6: Year 1 hourly PR

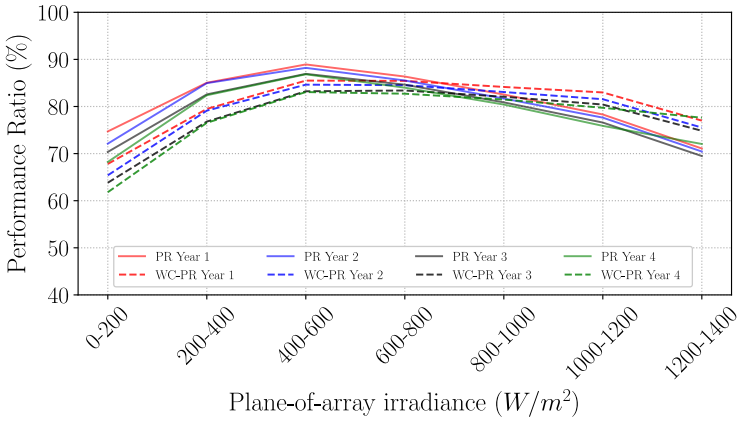

Figure 7: POA vs Performance Ratio

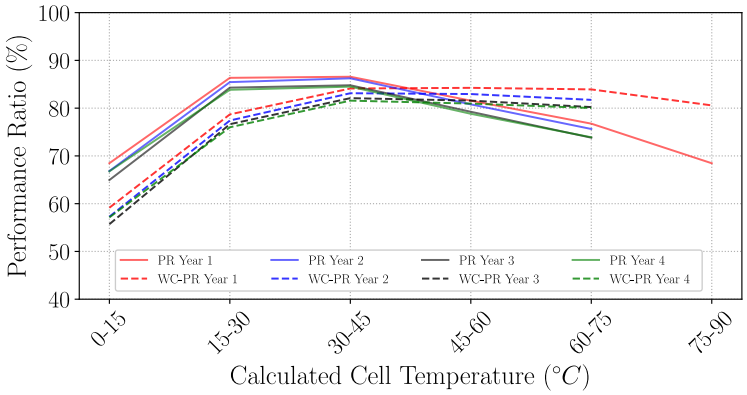

Figure 8: Calculated Cell Temperature vs Performance Ratio

Figure 9 shows the binned AM_a, mean measured POA irradiance and the associated PR calculations. AM is not binned in linear batches like with irradiance and temperature. The lower AM values have more stable WC-PR than normal PR. At lower AM values, the POA irradiance is the highest. From AM3, the PR starts to decline, as well as the irradiance. Higher AM values indicate timestamps closer to sunrise or sunset, where lower irradiance levels are expected.

In Figure 10, the higher PW levels indicate a decrease in PR. As the PW increases, the POA irradiance decreases, as expected, with a higher cloud content as a result of more water in the air. Similarly to the results seen in Figures 7 to 9, there is a period where the WC-PR is more stable than the normal PR. Stable WC-PR is noted for the POA irradiance, calculated cell temperature, AM, and PW for certain intervals. This is usually associated with ideal operating conditions, such as high irradiance (POA > 600 W/m^2), higher cell temperatures ($T_{cell,calc} > 30$℃), lower AM ($AM_a < 3$) and clearer skies where the PW is low ($PW < 0.8$ cm).

Lower irradiance levels are associated with either cloudy conditions or sunrise/sunset. Higher AM levels are associated with sunrise and sunset. The lower cell temperatures are associated with sunrise and sunset, where the PV power production is at a minimum. Higher PW levels are associated with clouds or moisture in the air. All these conditions are non-ideal performance climates.

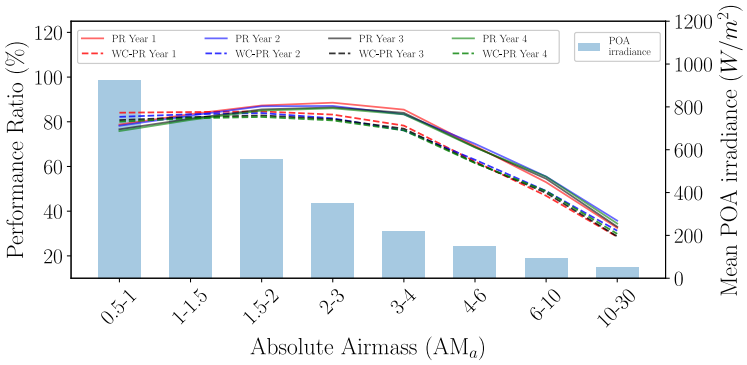

Figure 9: Absolute Airmass vs Performance Ratio and POA irradiance

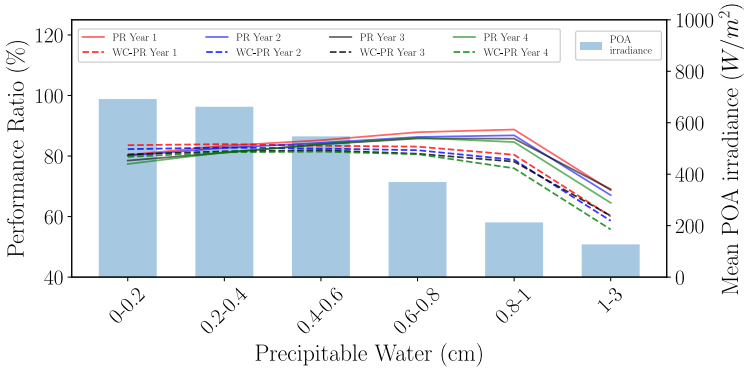

Figure 10: Precipitable Water vs Performance Ratio and POA irradiance

Figures 11 and 12 show the simulated spectral irradiance and the normalised spectral response (SR) for a polycrystalline PV module in various AM and PW scenarios. The simulated spectral irradiance is based on the work presented in (Bird & Riordan, 1986). The changes in spectral irradiance across the wavelengths are more pronounced for AMs that are different from those of PWs. The red and blue columns of the figures highlight significant changes in spectral irradiance, where the red also indicates the highest SR of the PV module.

The changes are noticeable in the 0.9 to 1 μm wavelengths, in particular, where the PV module should be able to best absorb the available spectral irradiance. PW levels below 1.42 cm (STC for PW) show a decrease in the difference from the STC spectrum, while PW values above 1.42 show an increase. Similarly, values below 1.5 AM show a decrease and those above show an increase in a change from STC in the spectral irradiance. The spectral irradiance indicates that the spectrum changes in a similar trend for PW and AM. When the light (spectral irradiance) increases, it passes through more water vapour and affects the spectrum in a similar way.

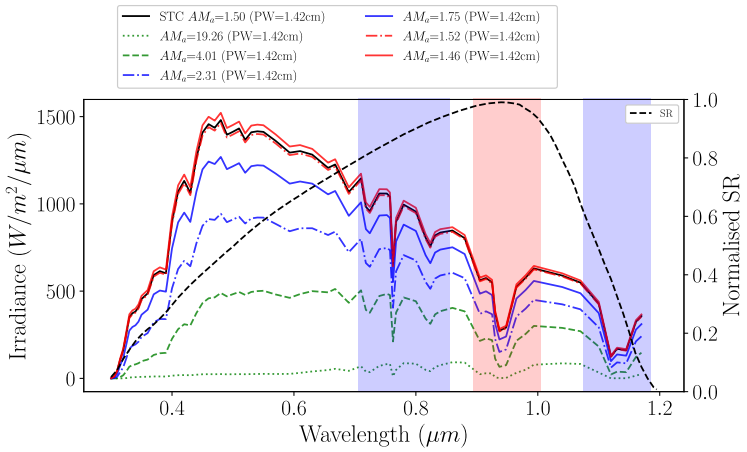

Figure 11: Simulated spectral irradiance and normalised SR for polycrystalline PV module for AM with constant PW

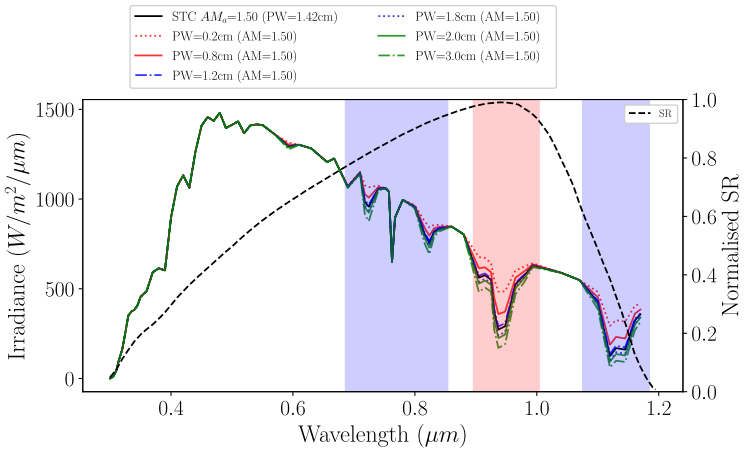

Figure 12: Simulated spectral irradiance and normalised SR for polycrystalline PV module for PW with constant AM

Figures 13 and 14 show the absolute normalised difference from STC. Both the AM and PW cause similar changes around the 0.9 to 1.0 μm wavelengths, with the AM's impact being more pronounced. The AM affects the wavelengths of 0.7 to 0.8 μm more compared to the PW. These effects are quite significant in the higher SR wavelengths of the polycrystalline PV module, which will then increase or decrease performance non-linearly.

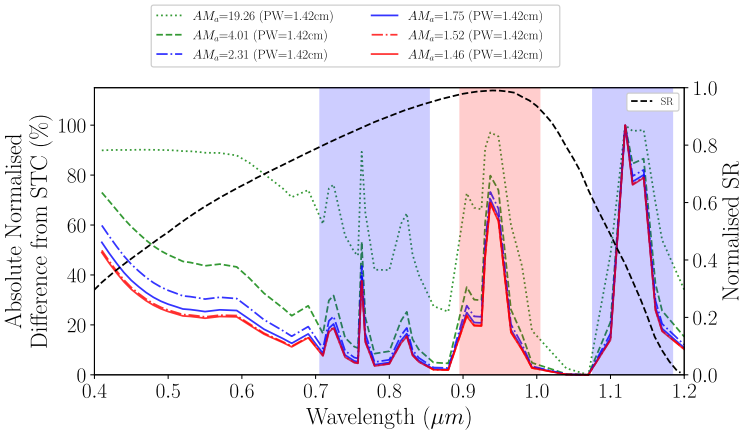

Figure 13: Absolute normalised difference from STC and normalised SR for polycrystalline PV module for AM with constant PW

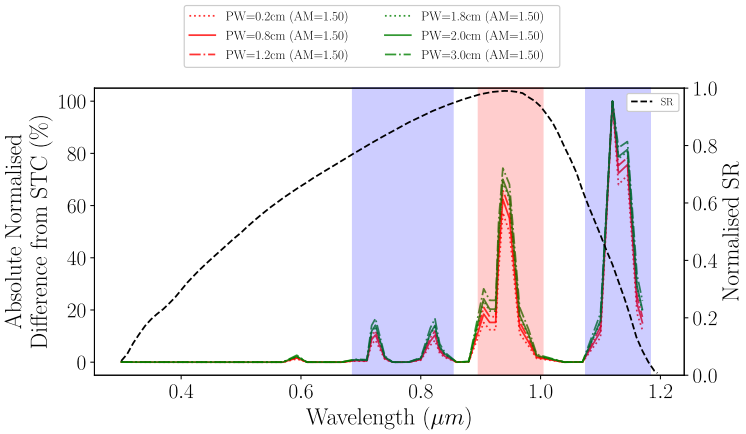

Figure 14: Absolute normalised difference from STC and normalised SR for polycrystalline PV module for PW with constant AM

5. Conclusion

This paper discusses the performance of a PV plant over 4 years by assessing the PR and WC-PR under well-known spectral influences. The WC-PR is stable for ideal operational circumstances and shows significant performance deterioration under non-ideal scenarios. For AM greater than 3, both PR and WC-PR show decreases in performance, and a similar trend was observed for PW greater than 0.8 cm. The lower calculated cell temperature and POA irradiance levels indicate underperformance as well. The results indicate that the spectrum has a considerable influence on the performance of PV modules, and at higher values of the PW and AM, the PR drops. Therefore, the conclusion can be drawn that if these spectral influences can be empirically defined, the PR can be corrected using AM and PW as spectral correction factors in the same way temperature and irradiance are used to improve the PR calculation.

References

Bird, R. E. & Riordan, C., 1986. Simple Solar Spectral Model for Direct and Diffuse Irradiance on Horizontal and Tilted Planes at the Earth's Surface for Cloudless Atmospheres. *Journal of Climate and Applied Meteorology,* Volume 25, pp. 87-97.

Caballero, J. A. et al., 2018. Spectral Corrections Based on Air Mass, Aerosol Optical Depth, and Precipitable Water for PV Performance Modeling. *IEEE Journal of Photovoltaics,* Volume 8, pp. 552-558.

Daher, D. H., Gaillard, L. & Ménézo, C., 2022. Experimental assessment of long-term performance degradation for a PV power plant operating in a desert maritime climate. *Renewable Energy,* Volume 187, pp. 44-55.

Dierauf, T. et al., 2013. *Weather-Corrected Performance Ratio,* Golden, Colorado: NREL.

Duck, B. C. & Fell, C. J., 2015. *Comparison of methods for estimating the impact of spectrum on PV output.* New Orleans, 2015 IEEE 42nd Photovoltaic Specialist Conference (PVSC), pp. 1-6.

Duck, B. C. & Fell, C. J., 2016. *Improving the spectral correction function.* Portland, 2016 IEEE 43rd Photovoltaic Specialists Conference (PVSC), pp. 2647-2652.

Gopi, A., Sudhakar, K., Keng, N. W. & Krishnan, A. R., 2021. Comparison of normal and weather corrected performance ratio of photovoltaic solar plants in hot and cold climates. *Energy for Sustainable Development,* Volume 65, pp. 53-62.

Gottschalg, R., Betts, T., Infield, D. & Kearney, M., 2004. On the importance of considering the incident spectrum when measuring the outdoor performance of amorphous silicon photovoltaic devices. *Measurement Science and Technology,* January, Volume 15, pp. 460-466.

Gouvêa, E. C., Sobrinho, P. M. & Souza, T. M., 2017. Spectral Response of Polycrystalline Silicon Photovoltaic Cells under Real-Use Conditions. *Energies,* Volume 10.

Gueymard, C., 1993. Assessment of the Accuracy and Computing Speed of Simplified Saturation Vapor Equations Using a New Reference Dataset. *Journal of Applied Meteorology,* June, Volume 32, pp. 1294-1300.

Gueymard, C., 1994. Analysis of monthly average atmospheric precipitable water and turbidity in Canada and Northern United States. *Solar Energy,* Volume 53, pp. 57-71.

International Electrotechnical Commission, 2021. *Photovoltaic system performance – Part 1: Monitoring,* Geneva: International Electrotechnical Commission.

Kasten, F. & Young, A. T., 1989. Revised optical air mass tables and approximation formula. *Appl. Opt.,* November, Volume 28, p. 4735–4738.

King, D., Kratochvil, J. & Boyson, W., 2004. *Photovoltaic Array Performance Model,* Albuquerque, New Mexico: SANDIA.

Lee, M. & Panchula, A., 2016. *Spectral correction for photovoltaic module performance based on air mass and precipitable water.* Portland, 2016 IEEE 43rd Photovoltaic Specialists Conference (PVSC), pp. 1351-1356.

Lewis, C., 2021. *Modelling Atmospheric Transmittance for Clear-Sky Spectral Solar Radiation in Practical Applications,* Stellebosch: Stellenbosch University.

Martin, N. C. & Ruiz, J., 1999. New method for the spectral characterization of PV modules. *Progress in Photovoltaics - PROG PHOTOVOLTAICS,* July, Volume 7, pp. 299-310.
Rodrigo, P. M. et al., 2019. Comparative assessment of simplified indexes for the spectral characterisation of photovoltaic systems. *Measurement,* Volume 133, pp. 1-8.
Solargis, 2022. © *2020 The World Bank, Source: Global Solar Atlas 2.0, Solar Resource Data: Solargis.* [Online] Available at: https://solargis.com/maps-and-gis-data/download/south-africa [Accessed 1 August 2022].